STRUCTURAL CHEMISTRY

ISSN: 2053-2296
journals.iucr.org/c

Crystal structures and Hirshfeld surface analysis of transition-metal complexes of 1,3-azolecarboxylic acids

Natthaya Meundaeng, Timothy John Prior and Apinpus Rujiwatra

Acta Cryst. (2019). C**75**, 1319–1326

Acta Cryst C STRUCTURAL CHEMISTRY
ISSN 2053-2296

Crystal structures and Hirshfeld surface analysis of transition-metal complexes of 1,3-azolecarboxylic acids

Natthaya Meundaeng,[a] Timothy John Prior[b] and Apinpus Rujiwatra[c,d]*

[a]Department of Chemistry, Faculty of Science, King Mongkut's Institute of Technology Ladkrabang, Bangkok, 10520, Thailand, [b]Department of Chemistry and Biochemistry, University of Hull, Kingston upon Hull, HU6 7RX, England, [c]Department of Chemistry, Faculty of Science, Chiang Mai University, Chiang Mai, 50200, Thailand, and [d]Materials Science Research Centre, Faculty of Science, Chiang Mai University, Chiang Mai, 50200, Thailand. *Correspondence e-mail: apinpus.rujiwatra@cmu.ac.th

Received 15 July 2019
Accepted 16 August 2019

Edited by P. Fanwick, Purdue University, USA

Keywords: transition metal; crystal structure; azolecarboxylic acid; Hirshfeld analysis; supramolecular interaction.

CCDC references: 1940482; 1940481; 1940480; 1940479; 1940478

Supporting information: this article has supporting information at journals.iucr.org/c

The crystal structures of five new transition-metal complexes synthesized using thiazole-2-carboxylic acid (2-Htza), imidazole-2-carboxylic acid (2-H_2ima) or 1,3-oxazole-4-carboxylic acid (4-Hoxa), namely diaquabis(thiazole-2-carboxylato-κ^2N,O)cobalt(II), $[Co(C_4H_2NO_2S)_2(H_2O)_2]$, **1**, diaquabis(thiazole-2-carboxylato-κ^2N,O)nickel(II), $[Ni(C_4H_2NO_2S)_2(H_2O)_2]$, **2**, diaquabis(thiazole-2-carboxylato-κ^2N,O)cadmium(II), $[Cd(C_4H_2NO_2S)_2(H_2O)_2]$, **3**, diaquabis(1*H*-imidazole-2-carboxylato-κ^2N^3,O)cobalt(II), $[Co(C_4H_2N_2O_2)_2(H_2O)_2]$, **4**, and diaquabis(1,3-oxazole-4-carboxylato-κ^2N,O^4)cobalt(II), $[Co(C_4H_2NO_3)_2(H_2O)_2]$, **5**, are reported. The influence of the nature of the heteroatom and the position of the carboxyl group in relation to the heteroatom on the self-assembly process are discussed based upon Hirshfeld surface analysis and used to explain the observed differences in the single-crystal structures and the supramolecular frameworks and topologies of complexes **1**–**5**.

1. Introduction

The understanding of the self-assembly process through both strong bonding (coordinative or covalent) and nonbonding interactions is a fundamental of crystal engineering (Seth *et al.*, 2011), since properties of crystalline materials strongly depend on how structural components are organized with respect to one another (Yu, 2002; Bis *et al.*, 2006). In contrast to the strong and directional bonding, the nature of nonbonding interactions, such as hydrogen bonding and aromatic π–π interactions, causes difficulties in crystal structure prediction (Braga *et al.*, 2002). Supramolecular assembly regulated through a diverse range of these interactions is often explained and rationalized using the concept of molecular synthons (Kitagawa & Uemura, 2005; Shimizu *et al.*, 2004), which have been well established for strong hydrogen bonds (Desiraju, 2002; Sherrington & Taskinen, 2001). The other weaker interactions, such as π–π, C—H$\cdots\pi$, lone pair–π and halogen interactions, nonetheless play a significant role in self-assembly processes (Blake *et al.*, 1999; Jayendran *et al.*, 2019). Despite being weaker individually, the accumulation of these very weak interactions can be as substantial as the covalent bond (Desiraju, 2005).

To acquire a greater understanding on how molecular components interact with their local environment, the molecular Hirshfeld surface analysis has been introduced to visualize and quantify the interplay of these nonbonded interactions (Spackman & Jayatilaka, 2009), which otherwise cannot be readily obtained from conventional structure

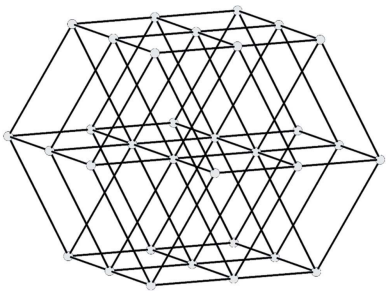

analysis. Similarities and differences between intermolecular interactions, as well as information on the relative strengths of these interactions in crystal packing, can be quantified (Clausen *et al.*, 2010; Wang *et al.*, 2018). Although this approach has been widely used in the study of the polymorphism of small molecules (Munshi *et al.*, 2010), it can also be useful for the investigation of interactions between different functionalities in supramolecular assemblies (Martin *et al.*, 2015). The changing of *tert*-butyl on *para*-substituted phenols to benzyl and nitro, for example, diversified the dominant interactions within the crystal packing and therefore the crystal structures (Martin *et al.*, 2010).

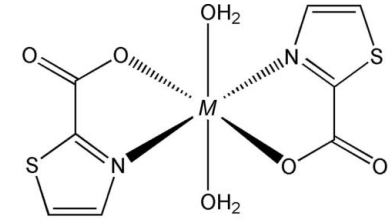

1 *M* = Co
2 *M* = Ni
3 *M* = Cd

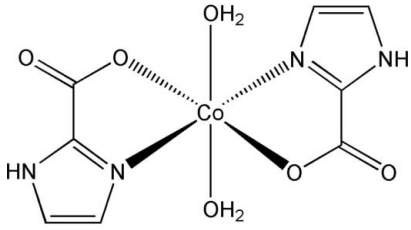

4

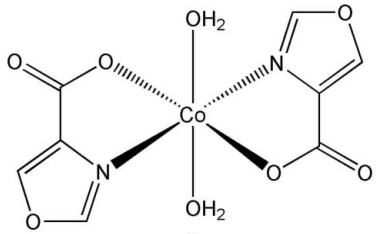

5

1,3-Azolecarboxylic acids, consisting of an azole ring and a carboxylic acid group, are an excellent choice of ligands owing to their structural adaptability to both the highly directional coordinative bonds, as well as the flexible nonbonding interactions (Sun *et al.*, 2010; Furuya *et al.*, 2001; Cheng *et al.*, 2014; Cai *et al.*, 2012; Rossin *et al.*, 2011, 2014; Meundaeng *et al.*, 2016, 2017). The effects of thiazole-4-carboxylate, for instance, on the variation of supramolecular structures and therefore polymorphism in Co^{2+} and Ni^{2+} complexes have been reported (Meundaeng *et al.*, 2016). Nevertheless, the effects of different heteroatoms, as well as the positions of the carboxylic acid group on the azole ring, on crystal packing has never been investigated.

Herein, the syntheses and single-crystal structures of five new metal complexes of thiazole-2-carboxylic acid (2-Htza), imidazole-2-carboxylic acid (2-H_2ima) and oxazole-4-carboxylic acid (4-Hoxa) (see Scheme), *i.e.* [*M*(2-tza)$_2$(H_2O)$_2$], where *M* = Co (**1**), Ni (**2**) and Cd (**3**), [Co(2-Hima)$_2$(H_2O)$_2$] (**4**) and [Co(4-oxa)$_2$(H_2O)$_2$] (**5**), are reported. A discussion of the differences and similarities in the nonbonding interactions and the supramolecular packing of the five crystal structures is presented based on Hirshfeld surface analyses.

2. Experimental

2.1. Materials and methods

Chemical reagents were purchased commercially and used as received without further purification; $CoCl_2·6H_2O$ (Fluka, 99.0%), $NiCl_2·6H_2O$ (Univar, 99.0%), $Cd(NO_3)_2·4H_2O$ (Sigma–Aldrich, 98%), $Co(NO_3)_2·6H_2O$ (Univar, 99.0%), $Ni(NO_3)_2·6H_2O$ (BDH Chemicals, 99.0%), thiazole-2-carboxylic acid (2-Htza; $C_4H_3NO_2S$, Sigma–Aldrich, 97%), imidazole-2-carboxylic acid (2-H_2ima; $C_4H_4N_2O_2$, Sigma–Aldrich, 98%) and oxazole-4-carboxylic acid (4-Hoxa; $C_4H_3NO_3$, Sigma–Aldrich, 97%).

2.2. Syntheses of 1–5

The syntheses of **1**–**5** followed a similar procedure. In the synthesis of **1**, $CoCl_2·2H_2O$ (0.0129 g, 0.100 mmol) and 2-Htza (0.0129 g, 0.100 mmol) were dissolved in distilled water (5.0 ml). The solution was left undisturbed at room temperature for several days, from which **1** crystallized. The same procedure was adopted for the syntheses of **2** and **3**, except that $NiCl_2·2H_2O$ (0.0129 g, 0.100 mmol) and $Cd(NO_3)_2·4H_2O$ (0.0129 g, 0.100 mmol), respectively, were used instead of $CoCl_2·2H_2O$. The procedure was also applied for the preparation of **4** and **5**, except that $Co(NO_3)_2·6H_2O$ (0.0290 g, 0.100 mmol) was used as a metal salt, whereas 2-H_2ima (0.0112 g, 0.100 mmol) and 4-Hoxa (0.0113 g, 0.100 mmol) were used as the ligands for the preparation of **4** and **5**, respectively.

2.3. Crystal structure determination

Crystal structure data for **1**–**5** are summarized in Table 1. All H atoms were refined freely and isotopically.

2.4. Hirshfeld surface analysis

The Hirshfeld surfaces and their associated two-dimensional (2D) fingerprint plots were analysed using *CrystalExplorer* software (Version 17.5; Spackman & Jayatilaka, 2009), based on the solved and refined single-crystal structures. All bond lengths to the H atoms were set to the default values (C—H = 1.083 Å, O—H = 0.983 Å and N—H = 1.009 Å) (Allen *et al.*, 1987). Graphical plots of the Hirshfeld surface were mapped with the normalized contact distance (d_{norm}) ranging from −0.5 to 1.0 Å. The red–white–blue colour scheme was adopted for presentation. Whilst red indicates the shorter intermolecular contacts, white shows the contacts around the van der Waals (vdW) radii separation and blue represents the longer contacts. To study the relative contributions of different intermolecular interactions in the crystal structures, the 2D fingerprint plots were created from the

Table 1
Experimental details.

For all structures: $Z = 2$. Experiments were carried out at 150 K with Mo $K\alpha$ radiation using a Stoe IPDS2 diffractometer. Absorption was corrected for by multi-scan methods (*SORTAV*; Blessing, 1995). All H-atom parameters were refined.

	1	**2**	**3**	**4**	**5**
Crystal data					
Chemical formula	$[Co(C_4H_2NO_2S)_2(H_2O)_2]$	$[Ni(C_4H_2NO_2S)_2(H_2O)_2]$	$[Cd(C_4H_2NO_2S)_2(H_2O)_2]$	$[Co(C_4H_2N_2O_2)_2(H_2O)_2]$	$[Co(C_4H_2NO_3)_2(H_2O)_2]$
M_r	351.21	350.99	404.68	317.13	319.09
Crystal system, space group	Monoclinic, $P2_1/n$	Monoclinic, $P2_1/n$	Monoclinic, $P2_1/n$	Monoclinic, $P2_1/c$	Monoclinic, $P2_1/c$
a, b, c (Å)	5.0481 (4), 18.633 (2), 6.7533 (6)	5.0710 (9), 18.239 (3), 6.8383 (17)	5.0198 (5), 19.052 (2), 6.8982 (7)	5.1145 (7), 10.6123 (12), 10.4179 (13)	5.1664 (7), 10.9879 (15), 9.7550 (11)
β (°)	109.517 (7)	109.780 (16)	109.281 (7)	97.858 (10)	99.378 (10)
V (Å^3)	598.73 (10)	595.2 (2)	622.71 (11)	560.14 (12)	546.37 (12)
μ (mm^{-1})	1.81	2.01	2.11	1.56	1.61
Crystal size (mm)	0.50 × 0.17 × 0.17	0.46 × 0.11 × 0.10	0.40 × 0.27 × 0.08	0.20 × 0.11 × 0.11	0.20 × 0.11 × 0.11
Data collection					
T_{min}, T_{max}	0.677, 0.720	0.817, 0.823	0.850, 0.914	0.944, 0.948	0.942, 0.948
No. of measured, independent and observed [$I > 2\sigma(I)$] reflections	4040, 1606, 1382	4011, 1594, 1367	4992, 1673, 1458	3303, 1495, 1078	2995, 1458, 1104
R_{int}	0.025	0.036	0.032	0.027	0.024
$(\sin\theta/\lambda)_{max}$ (Å^{-1})	0.685	0.685	0.685	0.686	0.686
Refinement					
$R[F^2 > 2\sigma(F^2)]$, $wR(F^2)$, S	0.022, 0.054, 0.97	0.022, 0.057, 0.95	0.019, 0.047, 1.00	0.023, 0.048, 0.84	0.025, 0.052, 0.91
No. of reflections	1606	1594	1673	1495	1458
No. of parameters	98	98	98	99	98
$\Delta\rho_{max}$, $\Delta\rho_{min}$ (e Å^{-3})	0.36, −0.28	0.50, −0.29	0.89, −0.84	0.32, −0.28	0.37, −0.28

Computer programs: *X-AREA* (Stoe & Cie, 2016), *SORTAV* (Blessing, 1987, 1989), *SHELXT2014* (Sheldrick, 2015*a*), *SHELXS86* (Sheldrick, 2008), *SHELXL2018* (Sheldrick, 2015*b*), *ORTEP-3* (Farrugia, 2012) and *DIAMOND* (Brandenburg & Berndt, 1999).

Hirshfeld surfaces. The colouring of each bin (essentially a pixel) of the resulting 2D histogram was presented as a function of the fraction of surface points in the particular bin, traversing from blue (few points) through green to red (many points). The plots were displayed in the standard 0.4–3.0 Å range for the scales of the d_e and d_i, axes, where d_i is the closest internal distance from a given point on the Hirshfeld surface and d_e is the closest contact point external to the surface.

3. Results and discussion

3.1. Description of the crystal structures

3.1.1. $[M(2\text{-tza})_2(H_2O)_2]$ (M = Co, 1, Ni, 2, and Cd, 3). Complexes **1**–**3** are isostructural and crystallize in the monoclinic space group $P2_1/n$. They are also isostructural with the previously reported compound $[Zn(2\text{-tza})_2(H_2O)_2]$ (Rossin *et al.*, 2011). The asymmetric unit of **1** (as a representative of **1**–**3**) contains one crystallographically unique Co^{2+} atom, a single thiazole-2-carboxylate (2-tza$^-$) anionic ligand and a water molecule (Fig. 1). The operation of the inversion centre located at Co^{2+} then completes the octahedral requirement, leading to the occupation of the equatorial plane by two equivalent 2-tza$^-$ ligands, with two water molecules at the axial positions. The 2-tza$^-$ ligand coordinates to Co^{2+} in an *N*,*O*-chelating mode, generating the five-membered chelate ring as expected. The Co1—N1 bond length in **1** is 2.1161 (12) Å, while the Co1—O1 and Co1—O3 bond lengths are 2.1191 (10) and 2.1082 (10) Å, respectively. These bond lengths are comparable to those of the Ni^{2+} and Cd^{2+} analogues, as well as those of the Zn^{2+} analogue (Rossin *et al.*, 2011).

Supramolecular assembly in the crystal structure of **1** is mainly directed by intermolecular hydrogen-bonding interactions, *i.e.* O—H···O, C—H···O and C—H···S (Table 2).

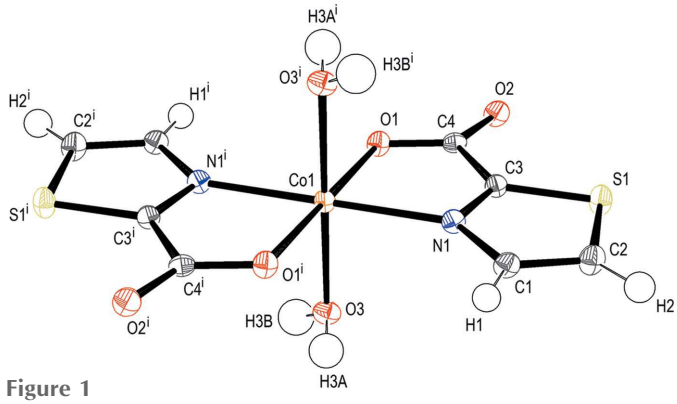

Figure 1
The molecular structure of **1**, showing atoms drawn as 50% probability displacement ellipsoids and the atom-labelling scheme. [Symmetry code: (i) $-x+1, -y+1, -z+1$.]

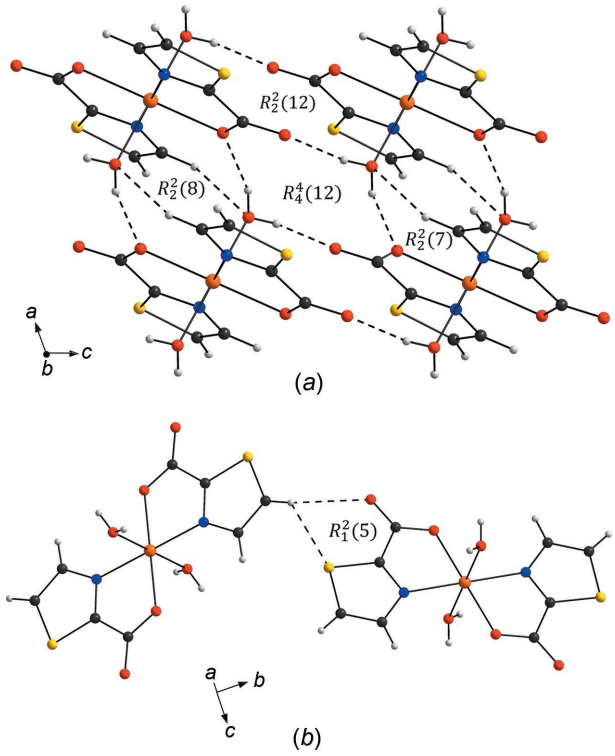

Figure 2
Views of (*a*) the 2D sheet of **1**, with hydrogen-bonding interactions shown as dashed lines, and (*b*) a bifurcated C—H···S hydrogen bond.

The O—H···O hydrogen bonds intriguingly form ring patterns of three different sizes, *i.e.* $R_4^4(12)$, $R_2^2(8)$ and $R_2^2(12)$ (Etter *et al.*, 1990), all of which involve the water O3 and carboxylate O1 and O2 atoms. These rings, together with the other $R_2^2(7)$ ring engaging the neighbouring aromatic C2 atom and the water O3 atom, result in the supramolecular arrangement of the molecules in a 2D sheet (Fig. 2*a*). The other type of hydrogen-bonded ring, which results in the three-dimensional (3D) supramolecular architecture (Fig. 3*a*), is the $R_1^2(5)$ ring (Fig. 2*b*). This ring involves a bifurcated hydrogen bond between the aromatic H1 atom, the thiazole S1 atom and the uncoordinated carboxylate O2 atom of the adjacent plane. In the cases of **2** and **3**, the hydrogen-bonding patterns are similar to those of **1**. The hydrogen-bond distances found in **2** (Ni^{2+}) are slightly shorter than those in **1** (Co^{2+}) and **3** (Cd^{2+}), which is attributed to the differences in the vdW radii of the metal ions. If the discrete [*M*(2-tza)$_2$(H$_2$O)$_2$] molecule is taken as a node, the hydrogen-bonding networks in these isostructural complexes **1**–**3** can be simplified to the 8-connected uninodal **bcu** (body-centred cubic) net, with a point symbol $4^{24}\cdot6^4$ (Fig. 3*b*) (Blatov *et al.*, 2014).

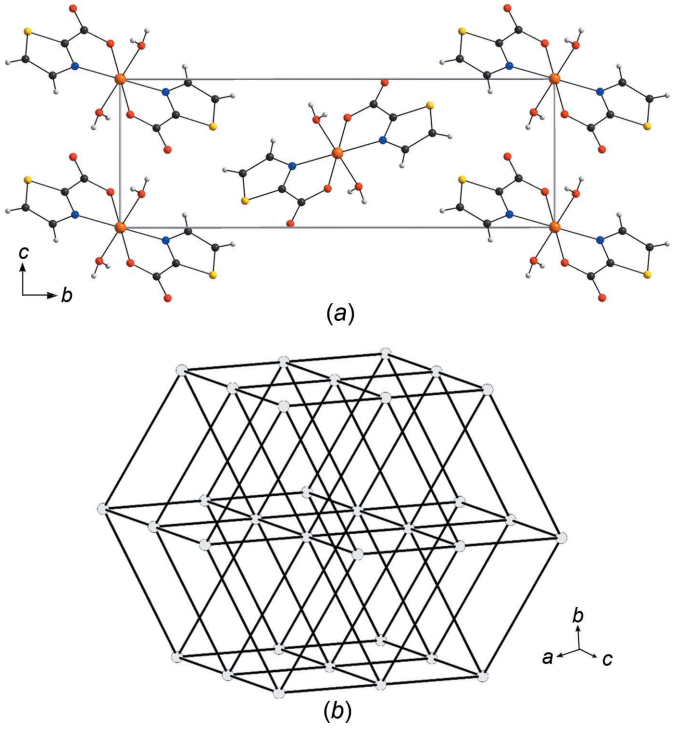

Figure 3
Views of (*a*) the molecular structure of **1** in the unit cell and (*b*) the simplified 8-connected uninodal **bcu** net.

Table 2
Table 2 Hydrogen-bond geometry (Å, °) for **1**–**5**.

D—H···*A*	*D*—H	H···*A*	*D*···*A*	*D*—H···*A*
1				
C2—H2···S1^{i}	0.94	2.69	3.3950 (15)	132
C2—H2···O2^{i}	0.94	2.63	3.3886 (18)	138
C1—H1···O3^{ii}	0.94	2.63	3.4140 (18)	140
O3—H3*A*···O2^{iii}	0.77 (2)	1.96 (2)	2.7158 (14)	168 (2)
O3—H3*B*···O1^{iv}	0.85 (3)	1.91 (3)	2.7326 (15)	161 (2)
2				
C2—H2···O3^{v}	0.97	2.60	3.4117 (19)	142
C1—H1···S1^{vi}	0.93	2.73	3.4060 (16)	131
C1—H1···O2^{vi}	0.93	2.60	3.346 (2)	138
O3—H3*A*···O2^{vii}	0.75 (2)	2.00 (2)	2.7345 (16)	166 (2)
O3—H3*B*···O1^{viii}	0.79 (3)	1.96 (3)	2.7388 (17)	168 (2)
3				
C3—H3···O3^{v}	0.94	2.66	3.4543 (19)	142
C4—H4···O1^{vi}	0.92	2.58	3.336 (2)	139
C4—H4···S1^{vi}	0.92	2.76	3.4218 (16)	130
O3—H3*B*···O2^{viii}	0.81 (3)	1.97 (3)	2.7294 (18)	157 (3)
O3—H3*A*···O1^{vii}	0.78 (3)	1.95 (3)	2.7106 (17)	165 (3)
4				
C1—H1···O2^{ix}	0.91	2.44	3.347 (2)	172
N2—H2*A*···O1^{x}	0.86	2.37	2.9824 (18)	129
N2—H2*A*···O3^{x}	0.86	2.20	2.978 (2)	151
O3—H3*A*···O2^{xi}	0.81 (2)	1.87 (2)	2.6731 (18)	168 (2)
O3—H3*B*···O1^{v}	0.78 (2)	1.92 (3)	2.6963 (17)	173 (2)
5				
C1—H1···O2^{ix}	0.93	2.27	3.1781 (19)	166
C2—H2···O3^{x}	0.85	2.50	3.238 (2)	146
O3—H3*A*···O2^{xi}	0.82 (3)	1.88 (3)	2.6949 (18)	178 (2)
O3—H3*B*···O1^{v}	0.76 (3)	1.98 (3)	2.7333 (16)	175 (3)

Symmetry codes: (i) $x+\frac{1}{2}, -y+\frac{3}{2}, z-\frac{1}{2}$; (ii) $x+1, y, z$; (iii) $x, y, z-1$; (iv) $-x, -y+1, -z+1$; (v) $x-1, y, z$; (vi) $x-\frac{1}{2}, -y+\frac{3}{2}, z+\frac{1}{2}$; (vii) $x, y, z+1$; (viii) $-x+2, -y+1, -z+1$; (ix) $x-1, -y+\frac{3}{2}, z+\frac{1}{2}$; (x) $-x+1, y+\frac{1}{2}, -z+\frac{1}{2}$; (xi) $-x+1, y-\frac{1}{2}, -z+\frac{1}{2}$.

3.1.2. [Co(2-Hima)$_2$(H$_2$O)$_2$] (4). The molecular structure of complex **4** is similar to those of **1**–**3**, crystallizing in the monoclinic space group $P2_1/c$. The asymmetric unit comprises half of the molecule built up of one each of the crystallographically unique Co^{2+} atom, an anionic 1*H*-imidazole-2-

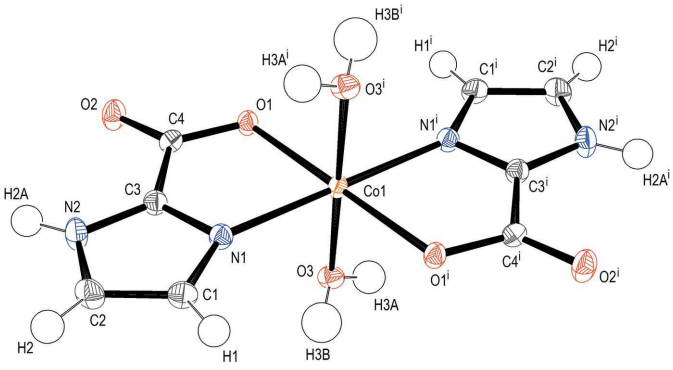

Figure 4
The molecular structure of **4**, showing atoms drawn as 50% probability displacement ellipsoids and the atom-labelling scheme. [Symmetry code: (i) $-x+1, -y+1, -z+1$.]

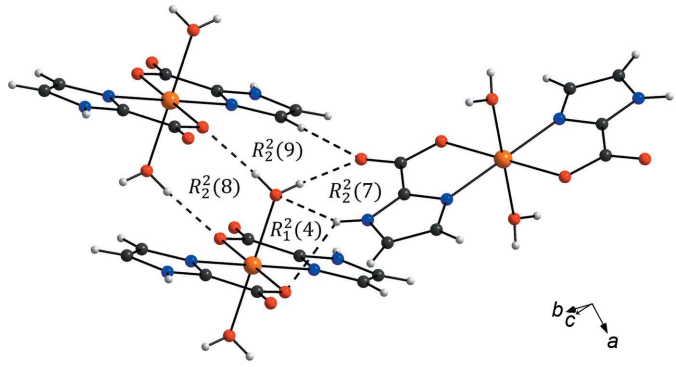

Figure 5
The hydrogen-bonded-ring patterns found in **4**.

carboxylate (2-Hima^{-}) ligand and a water molecule. The generation of the whole octahedral molecule occurs through the inversion centre located at Co^{2+} (Fig. 4). The arrangement of the ligands about the Co^{2+} centre is the same as those of **1**–**3**, and the same *N*,*O*-chelating coordination mode is adopted by 2-Hima^{-}. The Co1—N1 bond length in **4** is 2.1241 (13) Å, while the Co1—O1 and Co1—O3 bond lengths are 2.1041 (12) and 2.0931 (11) Å, respectively.

The 3D supramolecular packing of **4** is regulated by O—H···O, N—H···O and C—H···O hydrogen-bonding interactions (Table 2), which are organized into $R_1^2(4)$, $R_2^2(7)$, $R_2^2(8)$ and $R_2^2(9)$ hydrogen-bonded rings (Fig. 5). The involvement of the water O atom in every hydrogen-bonding pattern should be noted. In general, the patterns found in **4** conform to smaller rings than those in **1**–**3**. While the $R_2^2(7)$ and $R_2^2(8)$ motifs are common in every structure, the $R_1^2(4)$ and $R_2^2(9)$ motifs, featuring a bifurcated hydrogen bond, can only be found in **4**. Notably, these characteristic $R_1^2(4)$ and $R_2^2(9)$ patterns in **4** involve atoms on the azole ring. These hydrogen-bonding interactions connect the discrete [Co(2-Hima)$_2$(H$_2$O)$_2$] molecule into a 3D supramolecular network (Fig. 6*a*) which can be simplified to a 10-connected uninodal **bct** net with the point symbol $3^{12}\cdot4^{28}\cdot5^{5}$ (Fig. 6*b*) by taking the discrete unit as a node (Blatov *et al.*, 2014).

3.1.3. [Co(4-oxa)$_2$(H$_2$O)$_2$] (5). Complex **5** crystallizes in the same monoclinic space group $P2_1/c$ as **4** and possesses a similar asymmetric unit comprising one each of the crystallographically unique Co^{2+} atom, an anionic 1,3-oxazole-4-carboxylate (4-oxa^{-}) ligand and a water molecule (Fig. 7). By the operation of the inversion centre located on Co^{2+}, the whole octahedral molecule of [Co(4-oxa)$_2$(H$_2$O)$_2$] is generated, with a Co1—N1 bond length of 2.1476 (14) Å and Co1—O1 and Co1—O3 bond lengths of 2.0928 (11) and 2.0823 (14) Å, respectively. The 4-oxa^{-} ligand coordinates to the Co^{2+} atom also in an *N*,*O*-chelating mode, forming a five-membered ring.

The supramolecular packing in **5** is directed by O—H···O and C—H···O hydrogen–bonding interactions (Table 2). Based on the connectivity of these interactions, three different sizes of hydrogen-bonded rings, *i.e.* $R_1^2(4)$, $R_2^2(7)$, $R_2^2(8)$ and

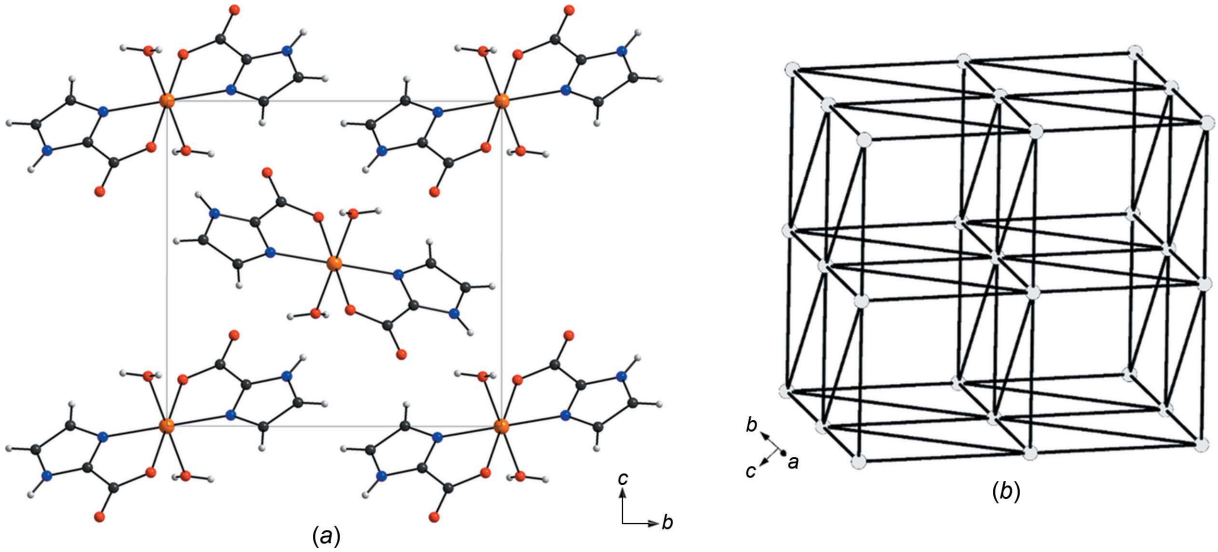

Figure 6
Views of (*a*) the molecular packing and (*b*) the simplified 8-connected uninodal **bct** net of **4**.

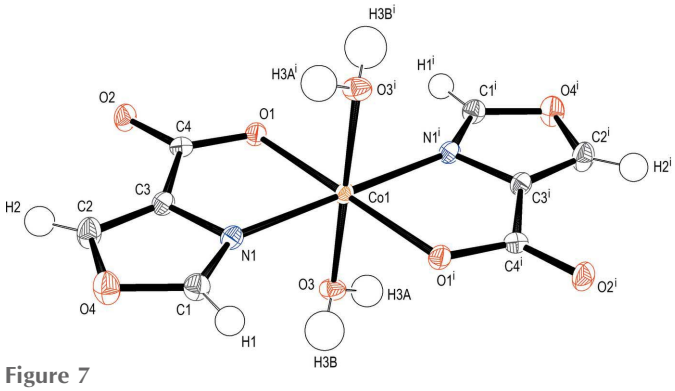

Figure 7
The molecular structure of **5**, showing atoms drawn as 50% probability displacement ellipsoids and the atom-labelling scheme. [Symmetry code: (i) $-x+1, -y+1, -z+1$.]

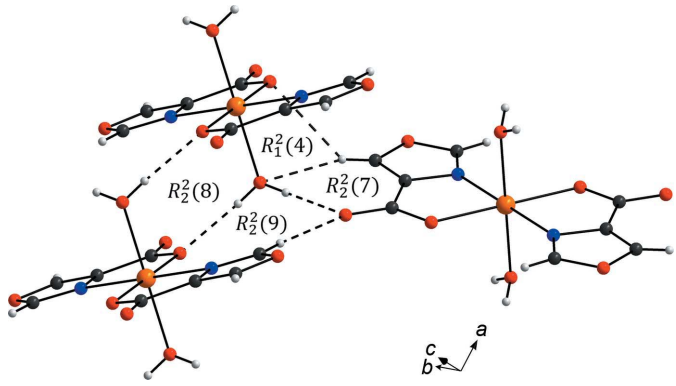

Figure 8
The hydrogen-bonded-ring patterns found in **5**.

$R_2^2(9)$, are formed (Fig. 8). They are very similar to those found in **4**. The fact that the water O atom is always part of the established hydrogen-bonding patterns is intriguingly common in every assembly, generating the $R_2^2(7)$ and $R_2^2(8)$ rings. The $R_1^2(4)$ and $R_2^2(9)$ rings in **5** are formed *via* the weak C—H···O interaction. The similarity in the hydrogen-bonding interaction patterns of **4** and **5** leads to very similar crystal packing and the same network topology of **bct** for both supramolecular arrangements (Blatov *et al.*, 2014).

3.2. Molecular structures of the ligands and supramolecular packing in cobalt complexes

Although the molecular structures of **1**, **4** and **5**, as well as the previously reported $[Co(4\text{-tza})_2(H_2O)_2]$ (Meundaeng *et al.*,

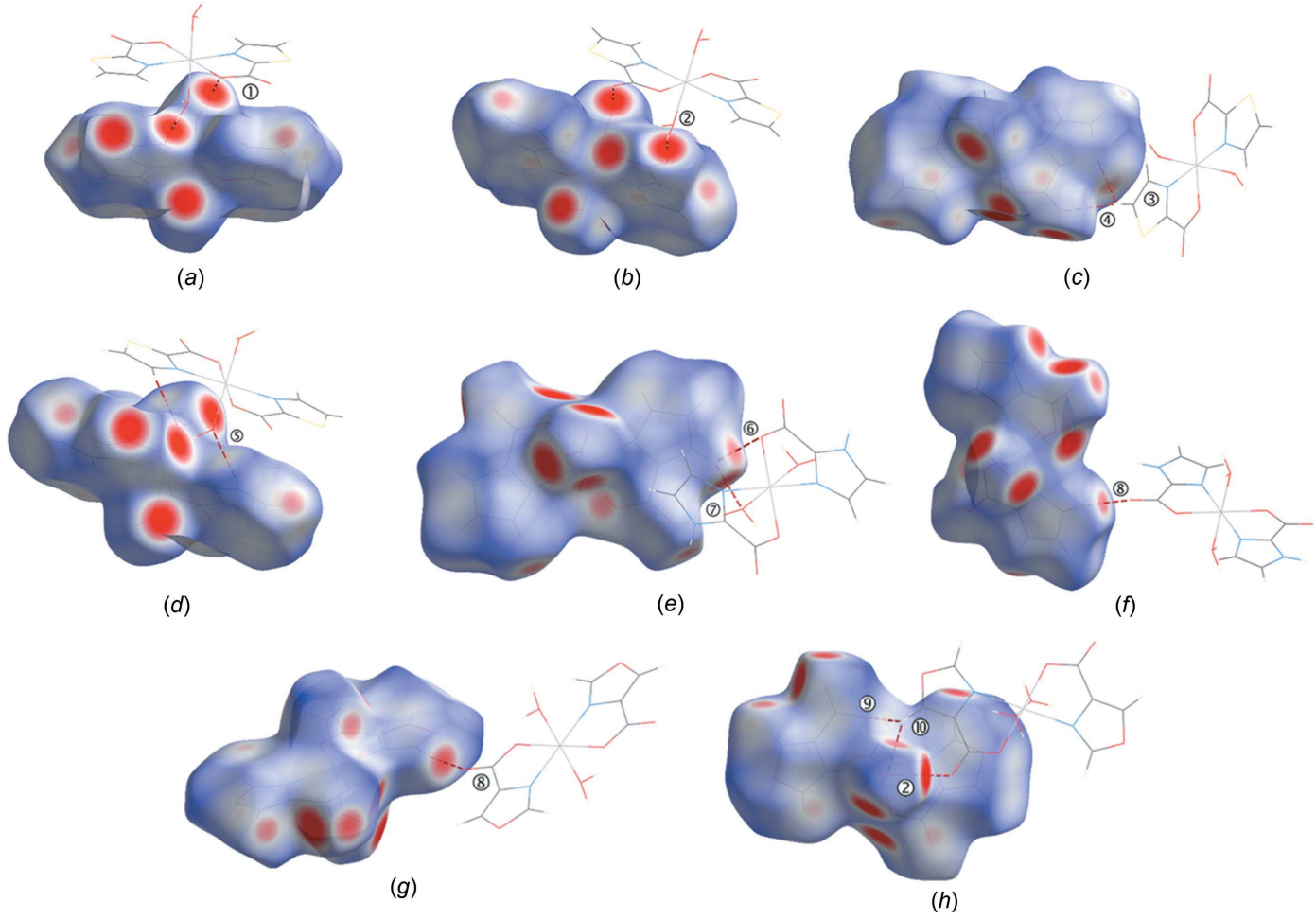

Figure 9
Hirshfeld surfaces of (*a*)–(*d*) **1**, (*e*)/(*f*) **4** and (*g*)/(*h*) **5**, viewed from different angles.

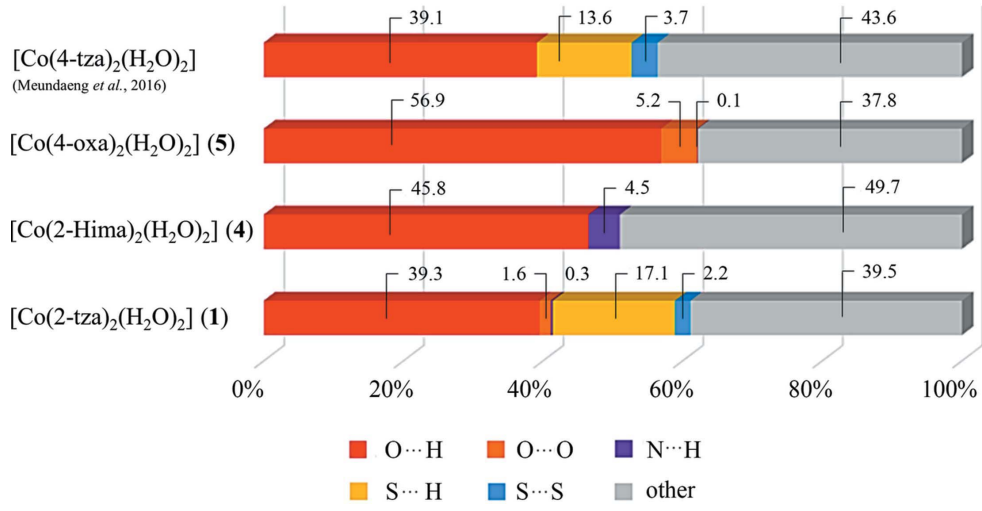

Figure 10
The relative contributions of important intermolecular contacts to the Hirshfeld surfaces of **1**, **4**, **5** and $[Co(4\text{-tza})_2(H_2O)_2]$.

2016), are alike, the packing of the molecular units in the crystal structures differs significantly. The apparent diversity in the crystal packing evidently derives from the differences in supramolecular interactions which stem from differences in the heteroatom of the ligand and the positions of the carboxylic acid group.

Whilst the S atom of 2-tza$^-$ in **1** acts as a hydrogen-bond acceptor, the N—H group of 2-Hima$^-$ in **4** functions as a hydrogen-bond donor. The diverse function of the heteroatoms, *i.e.* S and N—H, then leads to the establishment of smaller hydrogen-bonded rings in **4**, *i.e.* $R_2^2(9)$ and $R_1^2(4)$, compared with those found in **1**, *i.e.* $R_4^4(12)$, $R_2^2(12)$ and $R_1^2(5)$, in spite of their identical position in relation to the coordinating carboxylate group. The effect of the different heteroatoms on the supramolecular assembly in **5** (4-oxa$^-$) and $[Co(4\text{-tza})_2(H_2O)_2]$ (Meundaeng *et al.*, 2016) is nonetheless minimal since these heteroatoms are not involved in the hydrogen-bonding interactions.

The position of the carboxylic acid group relative to the heteroatom on the azole ring has a profound influence on the crystal packing though hydrogen-bond formation. As the carboxylate group of 2-tza$^-$ in **1**, for example, promotes the participation of the S atom in hydrogen-bond formation, that of 4-tza$^-$ in $[Co(4\text{-tza})_2(H_2O)_2]$ prevents the engagement of the S atom in hydrogen-bond interactions. The critical significance of the hydrogen-bond interactions in regulating the assembly process is also apparent.

3.3. Hirshfeld surface analysis

To gain a quantitative insight into the relative contribution of the hydrogen-bond interactions, the 3D Hirshfeld surfaces of the molecular units and the 2D fingerprint plots of any possible short interactions were established from the single-crystal data of **1** (as a representative of **1**–**3**), **4** and **5**. In each structure, the predominance of the O—H···O interactions, which are represented by the vivid red areas on the Hirshfeld surfaces, is evident (Fig. 9). The 2D fingerprint plots consistently showed the greatest percentages for the H···O/O···H contacts, accounting for *ca* 40 (**1**), 46 (**4**) and 57% (**5**) (Fig. S1–S3 in the supporting information). Apparently, the variation is in the other nonbonding interactions. The second strongest interactions in **1** are the C—H···S interactions, which contribute *ca* 17% for S···H/H···S contacts and the N—H···O interactions are the next biggest contributors in **4**, although the percentage is less than 5% for N···H/H···N contacts. These interactions are shown as pale-red areas on the Hirshfeld surfaces. Noticeably, there is a higher proportion of H···H contacts on the surface of **4** compared with **1**, which can be accounted for by the presence of the N—H group in the azole ring of 2-Hima$^-$ (**4**).

The Hirshfeld surface analysis of **1** can also be compared with that of $[Co(4\text{-tza})_2(H_2O)_2]$ (Meundaeng *et al.*, 2016), revealing the slightly smaller proportion of *ca* 14% for the H···S/S···H contacts and the higher proportion of *ca* 4% for the S···S contacts in $[Co(4\text{-tza})_2(H_2O)_2]$ (Fig. 10). The observed differences demonstrate the quantified influences due to the alteration of the carboxylate group from the 2-position (2-tza$^-$) to the 4-position (4-tza$^-$) on the thiazole ring.

The existence of O···H/H···O contacts in **5** is the most substantial among the reported complexes, accounting for *ca* 57% of the Hirshfeld surface, which is derived primarily from the higher proportion of O atoms in the molecular structure. Intriguingly, the azole O atom does not participate in these quantified O···H/H···O contacts. It interacts, on the other hand, with an aromatic O atom from an adjacent discrete molecule and ascribes to *ca* 5% of the O···O contacts on the surface. Compared with $[Co(4\text{-tza})_2(H_2O)_2]$ (Meundaeng *et al.*, 2016), the formation of the hydrogen-bond-ring patterns between these two crystal structures are very similar, resulting in the same crystal packing. However, it is evidenced from the Hirshfeld surface analyses that the fractional contribution of the intermolecular interactions involved in the solid-state assembly can be altered by changing the heteroatom on the azole ring (Fig. 10). This information is not readily apparent

from a conventional analysis of the crystal packing diagrams alone.

The Hirshfeld surface analyses not only provided 3D visualization of the nature and direction of all the possible nonbonding interactions present in the structures but also quantitative information on those interactions. These data then allowed a better understanding of the relationship between the supramolecular interactions and the self-assembling behaviours of the studied molecular structures.

4. Conclusions

Heterocyclic ligands, *i.e.* thiazole-2-carboxylate (2-tza$^-$), imidazole-2-carboxylate (2-Hima$^-$) and oxazole-4-carboxylate (4-oxa$^-$), provide a predictable chelating coordination mode to transition-metal ions. Although the molecular structures of the resulting complexes are relatively similar, the packing of the molecular units in their crystal structures, as well as the established nets for the hydrogen-bonding interactions, are significantly different, depending on the types of heteroatom and the positions of the carboxylate group in the ligand structures. Structural characterization also reveals that the solid-state assembly of the molecular structures is crucially governed by the hydrogen-bonding interactions, resulting in the 3D supramolecular architectures. The molecular Hirshfeld surfaces, the 2D fingerprint plots, as well as the enrichment ratios, have been used as tools to quantify these interactions, revealing the priority of these nonbonding interactions. Through the systematic variation in type of the heteroatom and position of the carboxylate group on 1,3-azolecarboxylic acids, the structure-directing features of these ligands through nonbonding interactions have been elucidated.

Acknowledgements

This work was funded by the Thailand Research Fund and Chiang Mai University. NM thanks the Science Achievement Scholarship of Thailand.

Funding information

Funding for this research was provided by: Thailand Research Fund (grant No. RSA6280003 to AR).

References

Allen, F. H., Kennard, O., Watson, D. G., Brammer, L., Orpen, A. G. & Taylor, R. (1987). *J. Chem. Soc. Perkin Trans. 2*, pp. S1–S19.
Bis, J. A., Vishweshwar, P., Middleton, R. A. & Zaworotko, M. J. (2006). *Cryst. Growth Des.* **6**, 1048–1053.
Blake, A. J., Champness, N. R., Hubberstey, P., Li, W.-S., Withersby, M. A. & Schröder, M. (1999). *Coord. Chem. Rev.* **183**, 117–138.
Blatov, V. A., Shevchenko, A. P. & Proserpio, D. M. (2014). *Cryst. Growth Des.* **14**, 3576–3586.
Blessing, R. H. (1987). *Crystallogr. Rev.* **1**, 3–58.
Blessing, R. H. (1989). *J. Appl. Cryst.* **22**, 396–397.
Blessing, R. H. (1995). *Acta Cryst.* A**51**, 33–38.
Braga, D., Desiraju, G. R., Miller, J. S., Orpen, A. G. & Price, S. L. (2002). *CrystEngComm*, **4**, 500–509.
Brandenburg, K. & Berndt, M. (1999). *DIAMOND*. Crystal Impact GbR, Bonn, Germany.
Cai, S.-L., Pan, M., Zheng, S.-R., Tan, J.-B., Fan, J. & Zhang, W.-G. (2012). *CrystEngComm*, **14**, 2308–2315.
Cheng, Y.-F., Lu, X.-M. & Wang, G. (2014). *Dalton Trans.* **43**, 5357–5363.
Clausen, H. F., Chevallier, M. S., Spackman, M. A. & Iversen, B. B. (2010). *New J. Chem.* **34**, 193–199.
Desiraju, G. R. (2002). *Acc. Chem. Res.* **35**, 565–573.
Desiraju, G. R. (2005). *Chem. Commun.* pp. 2995–3001.
Etter, M. C., MacDonald, J. C. & Bernstein, J. (1990). *Acta Cryst.* B**46**, 256–262.
Farrugia, L. J. (2012). *J. Appl. Cryst.* **45**, 849–854.
Furuya, F., Kobayashi, N., Bian, Y. & Jiang, J. (2001). *Chem. Lett.* **30**, 944–945.
Jayendran, M., Sithambaresan, M., Begum, P. M. S. & Kurup, M. R. P. (2019). *Polyhedron*, **158**, 386–397.
Kitagawa, S. & Uemura, K. (2005). *Chem. Soc. Rev.* **34**, 109–119.
Martin, A. D., Britton, J., Easun, T. L., Blake, A. J., Lewis, W. & Schröder, M. (2015). *Cryst. Growth Des.* **15**, 1697–1706.
Martin, A. D., Hartlieb, K. J., Sobolev, A. N. & Raston, C. L. (2010). *Cryst. Growth Des.* **10**, 5302–5306.
Meundaeng, N., Rujiwatra, A. & Prior, T. J. (2016). *Transition Met. Chem.* **41**, 783–793.
Meundaeng, N., Rujiwatra, A. & Prior, T. J. (2017). *J. Solid State Chem.* **245**, 138–145.
Munshi, P., Jelsch, C., Hathwar, V. R. & Guru Row, T. N. (2010). *Cryst. Growth Des.* **10**, 1516–1526.
Rossin, A., Di Credico, B., Giambastiani, G., Gonsalvi, L., Peruzzini, M. & Reginato, G. (2011). *Eur. J. Inorg. Chem.* **2011**, 539–548.
Rossin, A., Tuci, G., Giambastiani, G. & Peruzzini, M. (2014). *ChemPlusChem*, **79**, 406–412.
Seth, S. K., Sarkar, D., Roy, A. & Kar, T. (2011). *CrystEngComm*, **13**, 6728–6741.
Sheldrick, G. M. (2008). *Acta Cryst.* A**64**, 112–122.
Sheldrick, G. M. (2015*a*). *Acta Cryst.* A**71**, 3–8.
Sheldrick, G. M. (2015*b*). *Acta Cryst.* C**71**, 3–8.
Sherrington, D. C. & Taskinen, K. A. (2001). *Chem. Soc. Rev.* **30**, 83–93.
Shimizu, E., Kondo, M., Fuwa, Y., Sarker, R. P., Miyazawa, M., Ueno, M., Naito, T., Maeda, K. & Uchida, F. (2004). *Inorg. Chem. Commun.* **7**, 1191–1194.
Spackman, M. A. & Jayatilaka, D. (2009). *CrystEngComm*, **11**, 19–32.
Stoe & Cie (2016). *X-AREA*. Stoe & Cie GmbH, Darmstadt, Germany.
Sun, Y.-G., Guo, M.-Y., Xiong, G., Ding, F., Wang, L., Jiang, B., Zhu, M.-C., Gao, E.-J. & Verpoort, F. (2010). *J. Coord. Chem.* **63**, 4188–4200.
Wang, X., Xu, H.-J., Jia, X.-D., Yang, Y.-T. & Zhang, X.-J. (2018). *Acta Cryst.* C**74**, 381–385.
Yu, L. (2002). *J. Phys. Chem. A*, **106**, 544–550.

supporting information

Acta Cryst. (2019). C**75**, 1319-1326 [https://doi.org/10.1107/S2053229619011525]

Crystal structures and Hirshfeld surface analysis of transition-metal complexes of 1,3-azolecarboxylic acids

Natthaya Meundaeng, Timothy John Prior and Apinpus Rujiwatra

Computing details

For all structures, data collection: *X-AREA* (Stoe & Cie, 2016); cell refinement: *X-AREA* (Stoe & Cie, 2016); data reduction: *SORTAV* (Blessing, 1987, 1989). Program(s) used to solve structure: SHELXT2014 (Sheldrick, 2015a) for Co-2tza, Ni-2tza, Cd-2tza, Co-2Hima; *SHELXS86* (Sheldrick, 2008) for Co-4oxa. For all structures, program(s) used to refine structure: *SHELXL2018* (Sheldrick, 2015b).

Diaquabis(thiazole-2-carboxylato-κ^2N,O)cobalt(II) (Co-2tza)

Crystal data

$[Co(C_4H_2NO_2S)_2(H_2O)_2]$
M_r = 351.21
Monoclinic, $P2_1/n$
a = 5.0481 (4) Å
b = 18.633 (2) Å
c = 6.7533 (6) Å
β = 109.517 (7)°
V = 598.73 (10) Å^3
Z = 2
$F(000)$ = 354
D_x = 1.948 Mg m^{-3}
Mo $K\alpha$ radiation, λ = 0.71073 Å
Cell parameters from 4872 reflections
θ = 2.2–29.6°
μ = 1.81 mm^{-1}
T = 150 K
Block, dark pink
0.50 × 0.17 × 0.17 mm

Data collection

Stoe IPDS2 diffractometer
Radiation source: fine-focus sealed tube
Detector resolution: 6.67 pixels mm^{-1}
ω–scans
Absorption correction: multi-scan (SORTAV; Blessing, 1995)
T_{min} = 0.677, T_{max} = 0.720
4040 measured reflections
1606 independent reflections
1382 reflections with $I > 2\sigma(I)$
R_{int} = 0.025
θ_{max} = 29.2°, θ_{min} = 2.2°
h = −4→6
k = −25→22
l = −9→9

Refinement

Refinement on F^2
Least-squares matrix: full
$R[F^2 > 2\sigma(F^2)]$ = 0.022
$wR(F^2)$ = 0.054
S = 0.97
1606 reflections
98 parameters
0 restraints
Hydrogen site location: difference Fourier map
All H-atom parameters refined
$w = 1/[\sigma^2(F_o^2) + (0.0344P)^2]$ where $P = (F_o^2 + 2F_c^2)/3$
$(\Delta/\sigma)_{max} < 0.001$
$\Delta\rho_{max}$ = 0.36 e Å^{-3}
$\Delta\rho_{min}$ = −0.28 e Å^{-3}

Special details

Geometry. All esds (except the esd in the dihedral angle between two l.s. planes) are estimated using the full covariance matrix. The cell esds are taken into account individually in the estimation of esds in distances, angles and torsion angles; correlations between esds in cell parameters are only used when they are defined by crystal symmetry. An approximate (isotropic) treatment of cell esds is used for estimating esds involving l.s. planes.

Refinement. X-ray diffraction intensity data of 1</b->-5 were collected in the series of w-scans using Stoe IPDS2 image plate diffractometer operated with Mo Kα radiation at 150 (2) K. The multi-scan absorption corrections were applied for every collected data set (Blessing, 1987; Blessing, 1989). The structures were solved using dual-space methods within SHELXT and full-matrix least squares refinements were carried out within SHELXL-2018/3 via the WinGX program interface (Sheldrick, 2015). All non-hydrogen positions were located in the direct and the difference Fourier maps and refined using anisotropic displacement parameters.

Fractional atomic coordinates and isotropic or equivalent isotropic displacement parameters (Å²)

	x	*y*	*z*	U_{iso}*/U_{eq}
Co1	0.500000	0.500000	0.500000	0.01262 (8)
S1	0.68756 (8)	0.71302 (2)	0.82051 (5)	0.01889 (9)
O1	0.3270 (2)	0.52278 (5)	0.73902 (14)	0.0156 (2)
O3	0.1516 (2)	0.54862 (6)	0.27445 (14)	0.0173 (2)
O2	0.3324 (2)	0.60882 (6)	0.97625 (14)	0.0184 (2)
N1	0.6624 (2)	0.60438 (6)	0.58708 (15)	0.0138 (2)
C4	0.3988 (3)	0.58325 (7)	0.82967 (18)	0.0136 (3)
C3	0.5815 (3)	0.62785 (7)	0.74123 (18)	0.0136 (2)
C2	0.8481 (3)	0.71826 (8)	0.6352 (2)	0.0189 (3)
H2	0.946 (2)	0.7588 (9)	0.6121 (5)	0.023*
C1	0.8151 (3)	0.65571 (7)	0.52517 (19)	0.0157 (3)
H1	0.8902 (14)	0.64818 (16)	0.416 (2)	0.019*
H3A	0.188 (5)	0.5618 (11)	0.179 (3)	0.033 (5)*
H3B	−0.008 (5)	0.5279 (13)	0.240 (3)	0.038 (6)*

Atomic displacement parameters (Å²)

	U^{11}	U^{22}	U^{33}	U^{12}	U^{13}	U^{23}
Co1	0.01306 (13)	0.01334 (13)	0.01342 (12)	−0.00155 (10)	0.00703 (9)	−0.00072 (8)
S1	0.02500 (19)	0.01638 (16)	0.02084 (16)	−0.00498 (14)	0.01505 (13)	−0.00464 (11)
O1	0.0160 (5)	0.0157 (4)	0.0179 (4)	−0.0021 (4)	0.0093 (4)	−0.0004 (3)
O3	0.0155 (5)	0.0223 (5)	0.0157 (4)	−0.0021 (4)	0.0075 (4)	0.0024 (4)
O2	0.0233 (5)	0.0184 (5)	0.0185 (4)	0.0001 (4)	0.0136 (4)	0.0005 (4)
N1	0.0131 (5)	0.0152 (5)	0.0144 (5)	−0.0012 (4)	0.0064 (4)	0.0000 (4)
C4	0.0118 (6)	0.0157 (6)	0.0136 (5)	0.0016 (5)	0.0045 (4)	0.0027 (4)
C3	0.0138 (6)	0.0141 (6)	0.0139 (5)	−0.0011 (5)	0.0058 (4)	−0.0002 (4)
C2	0.0213 (7)	0.0178 (7)	0.0222 (6)	−0.0041 (6)	0.0135 (5)	−0.0008 (5)
C1	0.0170 (6)	0.0169 (6)	0.0161 (5)	−0.0009 (5)	0.0095 (5)	0.0012 (5)

Geometric parameters (Å, º)

Co1—O3	2.1082 (10)	O3—H3A	0.77 (2)
Co1—O3^{i}	2.1082 (10)	O3—H3B	0.85 (3)
Co1—N1^{i}	2.1161 (12)	O2—C4	1.2412 (16)

Co1—N1	2.1162 (12)	N1—C3	1.3138 (17)
Co1—O1^{i}	2.1191 (10)	N1—C1	1.3781 (18)
Co1—O1	2.1191 (10)	C4—C3	1.5052 (19)
S1—C3	1.7032 (14)	C2—C1	1.3622 (19)
S1—C2	1.7059 (15)	C2—H2	0.94 (2)
O1—C4	1.2757 (16)	C1—H1	0.945 (17)

O3—Co1—O3^{i}	180.0	Co1—O3—H3B	119.2 (15)
O3—Co1—N1^{i}	92.40 (4)	H3A—O3—H3B	112 (2)
O3^{i}—Co1—N1^{i}	87.59 (4)	C3—N1—C1	111.28 (11)
O3—Co1—N1	87.60 (4)	C3—N1—Co1	109.39 (9)
O3^{i}—Co1—N1	92.41 (4)	C1—N1—Co1	139.25 (9)
N1^{i}—Co1—N1	180.00 (6)	O2—C4—O1	127.78 (13)
O3—Co1—O1^{i}	89.57 (4)	O2—C4—C3	117.97 (12)
O3^{i}—Co1—O1^{i}	90.43 (4)	O1—C4—C3	114.24 (11)
N1^{i}—Co1—O1^{i}	79.87 (4)	N1—C3—C4	121.64 (12)
N1—Co1—O1^{i}	100.13 (4)	N1—C3—S1	114.26 (10)
O3—Co1—O1	90.43 (4)	C4—C3—S1	124.03 (10)
O3^{i}—Co1—O1	89.57 (4)	C1—C2—S1	110.47 (11)
N1^{i}—Co1—O1	100.13 (4)	C1—C2—H2	124.8
N1—Co1—O1	79.87 (4)	S1—C2—H2	124.8
O1^{i}—Co1—O1	180.00 (4)	C2—C1—N1	114.03 (12)
C3—S1—C2	89.96 (7)	C2—C1—H1	123.0
C4—O1—Co1	114.78 (9)	N1—C1—H1	123.0
Co1—O3—H3A	111.7 (16)		

Co1—O1—C4—O2	−178.41 (11)	O2—C4—C3—S1	−3.58 (17)
Co1—O1—C4—C3	2.76 (13)	O1—C4—C3—S1	175.38 (9)
C1—N1—C3—C4	176.82 (11)	C2—S1—C3—N1	0.48 (11)
Co1—N1—C3—C4	−0.53 (15)	C2—S1—C3—C4	−176.63 (11)
C1—N1—C3—S1	−0.37 (15)	C3—S1—C2—C1	−0.45 (11)
Co1—N1—C3—S1	−177.73 (6)	S1—C2—C1—N1	0.35 (16)
O2—C4—C3—N1	179.51 (12)	C3—N1—C1—C2	0.01 (17)
O1—C4—C3—N1	−1.54 (18)	Co1—N1—C1—C2	176.18 (10)

Symmetry code: (i) −*x*+1, −*y*+1, −*z*+1.

Hydrogen-bond geometry (Å, º)

D—H···*A*	*D*—H	H···*A*	*D*···*A*	*D*—H···*A*
C2—H2···S1^{ii}	0.94	2.69	3.3950 (15)	132
C2—H2···O2^{ii}	0.94	2.63	3.3886 (18)	138
C1—H1···O3^{iii}	0.94	2.63	3.4140 (18)	140
O3—H3*A*···O2^{iv}	0.77 (2)	1.96 (2)	2.7158 (14)	168 (2)
O3—H3*B*···O1^{v}	0.85 (3)	1.91 (3)	2.7326 (15)	161 (2)

Symmetry codes: (ii) *x*+1/2, −*y*+3/2, *z*−1/2; (iii) *x*+1, *y*, *z*; (iv) *x*, *y*, *z*−1; (v) −*x*, −*y*+1, −*z*+1.

Diaquabis(thiazole-2-carboxylato-κ^2N,O)nickel(II) (Ni-2tza)

Crystal data

$[Ni(C_4H_2NO_2S)_2(H_2O)_2]$
$M_r = 350.99$
Monoclinic, $P2_1/n$
$a = 5.0710$ (9) Å
$b = 18.239$ (3) Å
$c = 6.8383$ (17) Å
$\beta = 109.780$ (16)°
$V = 595.2$ (2) Å^3
$Z = 2$
$F(000) = 356$
$D_x = 1.959$ Mg m^{-3}
Mo $K\alpha$ radiation, $\lambda = 0.71073$ Å
Cell parameters from 4959 reflections
$\theta = 2.3$–$29.6°$
$\mu = 2.01$ mm^{-1}
$T = 150$ K
Block, blue
0.46 × 0.11 × 0.10 mm

Data collection

Stoe IPDS2 diffractometer
Radiation source: fine-focus sealed tube
Detector resolution: 6.67 pixels mm^{-1}
ω–scans
Absorption correction: multi-scan (SORTAV; Blessing, 1995)
$T_{min} = 0.817$, $T_{max} = 0.823$
4011 measured reflections
1594 independent reflections
1367 reflections with $I > 2\sigma(I)$
$R_{int} = 0.036$
$\theta_{max} = 29.1°$, $\theta_{min} = 2.2°$
$h = -6\rightarrow5$
$k = -21\rightarrow24$
$l = -9\rightarrow9$

Refinement

Refinement on F^2
Least-squares matrix: full
$R[F^2 > 2\sigma(F^2)] = 0.022$
$wR(F^2) = 0.057$
$S = 0.95$
1594 reflections
98 parameters
0 restraints
Hydrogen site location: difference Fourier map
All H-atom parameters refined
$w = 1/[\sigma^2(F_o^2) + (0.0372P)^2]$ where $P = (F_o^2 + 2F_c^2)/3$
$(\Delta/\sigma)_{max} = 0.001$
$\Delta\rho_{max} = 0.50$ e Å^{-3}
$\Delta\rho_{min} = -0.29$ e Å^{-3}

Special details

Geometry. All esds (except the esd in the dihedral angle between two l.s. planes) are estimated using the full covariance matrix. The cell esds are taken into account individually in the estimation of esds in distances, angles and torsion angles; correlations between esds in cell parameters are only used when they are defined by crystal symmetry. An approximate (isotropic) treatment of cell esds is used for estimating esds involving l.s. planes.

Refinement. X-ray diffraction intensity data of 1</b->-5 were collected in the series of w-scans using Stoe IPDS2 image plate diffractometer operated with Mo Kα radiation at 150 (2) K. The multi-scan absorption corrections were applied for every collected data set (Blessing, 1987; Blessing, 1989). The structures were solved using dual-space methods within SHELXT and full-matrix least squares refinements were carried out within SHELXL-2018/3 via the WinGX program interface (Sheldrick, 2015). All non-hydrogen positions were located in the direct and the difference Fourier maps and refined using anisotropic displacement parameters.

Fractional atomic coordinates and isotropic or equivalent isotropic displacement parameters (Å^2)

	x	y	z	U_{iso}*/U_{eq}
Ni1	0.500000	0.500000	0.500000	0.01278 (9)
S1	0.31739 (8)	0.71461 (2)	0.18386 (5)	0.01900 (10)
O3	0.8408 (2)	0.54992 (7)	0.72103 (16)	0.0170 (2)
O1	0.6774 (2)	0.52045 (6)	0.26838 (15)	0.0159 (2)
O2	0.6738 (2)	0.60702 (6)	0.03003 (15)	0.0190 (2)

N1	0.3413 (3)	0.60338 (7)	0.41318 (17)	0.0142 (2)
C4	0.6066 (3)	0.58173 (8)	0.1758 (2)	0.0137 (3)
C3	0.4232 (3)	0.62756 (8)	0.2609 (2)	0.0141 (3)
C2	0.1889 (3)	0.65508 (9)	0.4749 (2)	0.0161 (3)
H2	0.1120 (14)	0.64669 (18)	0.584 (2)	0.019*
C1	0.1560 (3)	0.71949 (9)	0.3671 (2)	0.0188 (3)
H1	0.060 (2)	0.7600 (10)	0.3898 (6)	0.023*
H3A	0.811 (5)	0.5601 (13)	0.818 (3)	0.036 (6)*
H3B	0.988 (6)	0.5304 (14)	0.742 (3)	0.037 (6)*

Atomic displacement parameters (Å²)

	U^{11}	U^{22}	U^{33}	U^{12}	U^{13}	U^{23}
Ni1	0.01260 (14)	0.01343 (14)	0.01475 (12)	0.00166 (10)	0.00782 (9)	0.00072 (9)
S1	0.0242 (2)	0.0168 (2)	0.02135 (17)	0.00458 (15)	0.01470 (15)	0.00453 (13)
O3	0.0141 (5)	0.0222 (6)	0.0172 (5)	0.0019 (5)	0.0084 (4)	−0.0026 (4)
O1	0.0160 (5)	0.0162 (5)	0.0187 (5)	0.0016 (4)	0.0102 (4)	0.0005 (4)
O2	0.0235 (6)	0.0192 (5)	0.0196 (5)	−0.0005 (5)	0.0143 (4)	−0.0010 (4)
N1	0.0135 (6)	0.0155 (6)	0.0151 (5)	0.0009 (5)	0.0068 (4)	0.0000 (4)
C4	0.0113 (7)	0.0154 (7)	0.0155 (5)	−0.0014 (5)	0.0057 (5)	−0.0032 (5)
C3	0.0129 (7)	0.0151 (7)	0.0150 (5)	0.0000 (5)	0.0057 (5)	0.0000 (5)
C2	0.0161 (7)	0.0175 (7)	0.0175 (6)	0.0011 (6)	0.0095 (5)	−0.0007 (5)
C1	0.0200 (7)	0.0188 (7)	0.0223 (6)	0.0035 (6)	0.0132 (6)	0.0000 (5)

Geometric parameters (Å, º)

Ni1—N1^{i}	2.0572 (13)	O3—H3B	0.79 (3)
Ni1—N1	2.0573 (13)	O1—C4	1.2748 (18)
Ni1—O3	2.0814 (12)	O2—C4	1.2460 (17)
Ni1—O3^{i}	2.0814 (12)	N1—C3	1.3207 (18)
Ni1—O1	2.1029 (11)	N1—C2	1.3728 (19)
Ni1—O1^{i}	2.1029 (11)	C4—C3	1.506 (2)
S1—C3	1.7013 (15)	C2—C1	1.367 (2)
S1—C1	1.7155 (15)	C2—H2	0.967 (18)
O3—H3A	0.75 (2)	C1—H1	0.93 (2)
N1^{i}—Ni1—N1	180.0	H3A—O3—H3B	114 (2)
N1^{i}—Ni1—O3	92.51 (5)	C4—O1—Ni1	114.14 (9)
N1—Ni1—O3	87.49 (5)	C3—N1—C2	111.89 (13)
N1^{i}—Ni1—O3^{i}	87.49 (5)	C3—N1—Ni1	109.69 (10)
N1—Ni1—O3^{i}	92.51 (5)	C2—N1—Ni1	138.31 (10)
O3—Ni1—O3^{i}	180.00 (5)	O2—C4—O1	127.90 (14)
N1^{i}—Ni1—O1	98.90 (4)	O2—C4—C3	118.40 (13)
N1—Ni1—O1	81.11 (4)	O1—C4—C3	113.69 (12)
O3—Ni1—O1	90.43 (5)	N1—C3—C4	121.29 (13)
O3^{i}—Ni1—O1	89.57 (5)	N1—C3—S1	113.92 (11)
N1^{i}—Ni1—O1^{i}	81.10 (4)	C4—C3—S1	124.72 (11)
N1—Ni1—O1^{i}	98.89 (4)	C1—C2—N1	113.80 (13)

O3—Ni1—O1^{i}	89.57 (5)	C1—C2—H2	123.1
O3^{i}—Ni1—O1^{i}	90.43 (5)	N1—C2—H2	123.1
O1—Ni1—O1^{i}	180.00 (6)	C2—C1—S1	110.35 (12)
C3—S1—C1	90.04 (7)	C2—C1—H1	124.8
Ni1—O3—H3A	112.4 (18)	S1—C1—H1	124.8
Ni1—O3—H3B	115.8 (18)		

Symmetry code: (i) −*x*+1, −*y*+1, −*z*+1.

Hydrogen-bond geometry (Å, º)

D—H···*A*	*D*—H	H···*A*	*D*···*A*	*D*—H···*A*
C2—H2···O3^{ii}	0.97	2.60	3.4117 (19)	142
C1—H1···S1^{iii}	0.93	2.73	3.4060 (16)	131
C1—H1···O2^{iii}	0.93	2.60	3.346 (2)	138
O3—H3*A*···O2^{iv}	0.75 (2)	2.00 (2)	2.7345 (16)	166 (2)
O3—H3*B*···O1^{v}	0.79 (3)	1.96 (3)	2.7388 (17)	168 (2)

Symmetry codes: (ii) *x*−1, *y*, *z*; (iii) *x*−1/2, −*y*+3/2, *z*+1/2; (iv) *x*, *y*, *z*+1; (v) −*x*+2, −*y*+1, −*z*+1.

Diaquabis(thiazole-2-carboxylato-κ^2N,O)cadmium(II) (Cd-2tza)

Crystal data

$[Cd(C_4H_2NO_2S)_2(H_2O)_2]$
M_r = 404.68
Monoclinic, $P2_1/n$
a = 5.0198 (5) Å
b = 19.052 (2) Å
c = 6.8982 (7) Å
β = 109.281 (7)°
V = 622.71 (11) Å^3
Z = 2
$F(000)$ = 396
D_x = 2.158 Mg m^{-3}
Mo $K\alpha$ radiation, λ = 0.71073 Å
Cell parameters from 5602 reflections
θ = 2.2–29.6°
μ = 2.11 mm^{-1}
T = 150 K
Block, colourless
0.40 × 0.27 × 0.08 mm

Data collection

Stoe IPDS2 diffractometer
Radiation source: fine-focus sealed tube
Detector resolution: 6.67 pixels mm^{-1}
ω scans
Absorption correction: multi-scan (SORTAV; Blessing, 1995)
T_{min} = 0.850, T_{max} = 0.914
4992 measured reflections
1673 independent reflections
1458 reflections with $I > 2\sigma(I)$
R_{int} = 0.032
θ_{max} = 29.2°, θ_{min} = 2.1°
h = −6→5
k = −25→22
l = −9→9

Refinement

Refinement on F^2
Least-squares matrix: full
$R[F^2 > 2\sigma(F^2)]$ = 0.019
$wR(F^2)$ = 0.047
S = 1.00
1673 reflections
98 parameters
0 restraints
Hydrogen site location: difference Fourier map
All H-atom parameters refined
$w = 1/[\sigma^2(F_o^2) + (0.0313P)^2]$ where $P = (F_o^2 + 2F_c^2)/3$
$(\Delta/\sigma)_{max}$ = 0.001
$\Delta\rho_{max}$ = 0.89 e Å^{-3}
$\Delta\rho_{min}$ = −0.84 e Å^{-3}

Special details

Geometry. All esds (except the esd in the dihedral angle between two l.s. planes) are estimated using the full covariance matrix. The cell esds are taken into account individually in the estimation of esds in distances, angles and torsion angles; correlations between esds in cell parameters are only used when they are defined by crystal symmetry. An approximate (isotropic) treatment of cell esds is used for estimating esds involving l.s. planes.

Refinement. X-ray diffraction intensity data of 1</b->-5 were collected in the series of w-scans using Stoe IPDS2 image plate diffractometer operated with Mo Kα radiation at 150 (2) K. The multi-scan absorption corrections were applied for every collected data set (Blessing, 1987; Blessing, 1989). The structures were solved using dual-space methods within SHELXT and full-matrix least squares refinements were carried out within SHELXL-2018/3 via the WinGX program interface (Sheldrick, 2015). All non-hydrogen positions were located in the direct and the difference Fourier maps and refined using anisotropic displacement parameters.

Fractional atomic coordinates and isotropic or equivalent isotropic displacement parameters (Å²)

	x	*y*	*z*	U_{iso}*/U_{eq}
Cd1	0.500000	0.500000	0.500000	0.01528 (6)
O3	0.8802 (3)	0.55617 (7)	0.73796 (17)	0.0194 (2)
O1	0.6482 (3)	0.61418 (7)	0.00368 (17)	0.0201 (2)
O2	0.6718 (2)	0.52899 (6)	0.23548 (16)	0.0178 (2)
C1	0.5919 (3)	0.58753 (8)	0.1499 (2)	0.0148 (3)
C2	0.4098 (3)	0.63096 (8)	0.2408 (2)	0.0140 (3)
C3	0.1748 (3)	0.66018 (9)	0.4519 (2)	0.0166 (3)
H3	0.1000 (15)	0.65356 (16)	0.559 (2)	0.020*
C4	0.1409 (3)	0.72058 (9)	0.3421 (2)	0.0191 (3)
H4	0.045 (3)	0.7595 (10)	0.3626 (6)	0.023*
N1	0.3275 (3)	0.60944 (7)	0.39317 (18)	0.0146 (2)
S1	0.30263 (9)	0.71402 (2)	0.16011 (6)	0.01898 (9)
H3B	1.012 (6)	0.5294 (17)	0.779 (4)	0.038 (7)*
H3A	0.839 (5)	0.5707 (14)	0.830 (4)	0.036 (7)*

Atomic displacement parameters (Å²)

	U^{11}	U^{22}	U^{33}	U^{12}	U^{13}	U^{23}
Cd1	0.01881 (9)	0.01293 (9)	0.01618 (8)	0.00218 (6)	0.00860 (6)	0.00253 (5)
O3	0.0198 (6)	0.0220 (6)	0.0183 (5)	0.0032 (5)	0.0091 (4)	−0.0017 (4)
O1	0.0282 (6)	0.0172 (6)	0.0211 (5)	0.0008 (5)	0.0167 (5)	0.0002 (4)
O2	0.0209 (6)	0.0164 (6)	0.0197 (5)	0.0038 (5)	0.0115 (4)	0.0016 (4)
C1	0.0147 (7)	0.0152 (7)	0.0160 (6)	−0.0011 (6)	0.0071 (5)	−0.0031 (5)
C2	0.0148 (7)	0.0141 (7)	0.0140 (6)	0.0007 (6)	0.0061 (5)	−0.0003 (5)
C3	0.0192 (7)	0.0166 (8)	0.0172 (6)	0.0007 (6)	0.0103 (6)	−0.0020 (5)
C4	0.0236 (8)	0.0165 (8)	0.0217 (7)	0.0041 (6)	0.0136 (6)	−0.0002 (5)
N1	0.0166 (6)	0.0140 (6)	0.0154 (5)	0.0010 (5)	0.0082 (5)	0.0007 (4)
S1	0.0263 (2)	0.01547 (19)	0.02063 (17)	0.00447 (16)	0.01507 (14)	0.00441 (14)

Geometric parameters (Å, º)

Cd1—N1	2.2845 (14)	O2—C1	1.264 (2)
Cd1—N1^{i}	2.2845 (14)	C1—C2	1.514 (2)
Cd1—O3	2.3267 (13)	C2—N1	1.3153 (18)

Cd1—O3^{i}	2.3268 (13)	C2—S1	1.7046 (16)
Cd1—O2	2.3276 (11)	C3—C4	1.357 (2)
Cd1—O2^{i}	2.3277 (11)	C3—N1	1.375 (2)
O3—H3B	0.81 (3)	C3—H3	0.944 (19)
O3—H3A	0.78 (3)	C4—S1	1.7098 (15)
O1—C1	1.2422 (18)	C4—H4	0.92 (2)
N1—Cd1—N1^{i}	180.00 (7)	C1—O2—Cd1	115.67 (9)
N1—Cd1—O3	86.74 (5)	O1—C1—O2	128.16 (14)
N1^{i}—Cd1—O3	93.26 (5)	O1—C1—C2	116.32 (14)
N1—Cd1—O3^{i}	93.26 (5)	O2—C1—C2	115.51 (12)
N1^{i}—Cd1—O3^{i}	86.74 (5)	N1—C2—C1	123.54 (14)
O3—Cd1—O3^{i}	180.00 (6)	N1—C2—S1	113.69 (11)
N1—Cd1—O2	74.31 (4)	C1—C2—S1	122.73 (11)
N1^{i}—Cd1—O2	105.69 (4)	C4—C3—N1	114.24 (13)
O3—Cd1—O2	90.80 (4)	C4—C3—H3	122.9
O3^{i}—Cd1—O2	89.20 (4)	N1—C3—H3	122.9
N1—Cd1—O2^{i}	105.69 (4)	C3—C4—S1	110.22 (12)
N1^{i}—Cd1—O2^{i}	74.31 (4)	C3—C4—H4	124.9
O3—Cd1—O2^{i}	89.20 (4)	S1—C4—H4	124.9
O3^{i}—Cd1—O2^{i}	90.80 (4)	C2—N1—C3	111.66 (13)
O2—Cd1—O2^{i}	180.0	C2—N1—Cd1	110.90 (10)
Cd1—O3—H3B	110 (2)	C3—N1—Cd1	137.32 (10)
Cd1—O3—H3A	111.1 (19)	C2—S1—C4	90.19 (8)
H3B—O3—H3A	110 (3)		

Symmetry code: (i) −*x*+1, −*y*+1, −*z*+1.

Hydrogen-bond geometry (Å, º)

D—H···*A*	*D*—H	H···*A*	*D*···*A*	*D*—H···*A*
C3—H3···O3^{ii}	0.94	2.66	3.4543 (19)	142
C4—H4···O1^{iii}	0.92	2.58	3.336 (2)	139
C4—H4···S1^{iii}	0.92	2.76	3.4218 (16)	130
O3—H3*B*···O2^{iv}	0.81 (3)	1.97 (3)	2.7294 (18)	157 (3)
O3—H3*A*···O1^{v}	0.78 (3)	1.95 (3)	2.7106 (17)	165 (3)

Symmetry codes: (ii) *x*−1, *y*, *z*; (iii) *x*−1/2, −*y*+3/2, *z*+1/2; (iv) −*x*+2, −*y*+1, −*z*+1; (v) *x*, *y*, *z*+1.

Diaquabis(1*H*-imidazole-2-carboxylato-κ^2N^3,O)cobalt(II) (Co-2Hima)

Crystal data

$[Co(C_4H_2N_2O_2)_2(H_2O)_2]$	*F*(000) = 322
M_r = 317.13	D_x = 1.880 Mg m^{-3}
Monoclinic, $P2_1/c$	Mo *Kα* radiation, λ = 0.71073 Å
a = 5.1145 (7) Å	Cell parameters from 2611 reflections
b = 10.6123 (12) Å	θ = 2.8–29.5°
c = 10.4179 (13) Å	μ = 1.56 mm^{-1}
β = 97.858 (10)°	*T* = 150 K
V = 560.14 (12) Å^3	Block, pale orange
Z = 2	0.20 × 0.11 × 0.11 mm

Data collection

Stoe IPDS2
diffractometer
Radiation source: fine-focus sealed tube
Detector resolution: 6.67 pixels mm^{-1}
ω–scans
Absorption correction: multi-scan
(SORTAV; Blessing, 1995)
T_{min} = 0.944, T_{max} = 0.948

3303 measured reflections
1495 independent reflections
1078 reflections with $I > 2\sigma(I)$
R_{int} = 0.027
θ_{max} = 29.2°, θ_{min} = 2.8°
h = −6→7
k = −13→14
l = −14→13

Refinement

Refinement on F^2
Least-squares matrix: full
$R[F^2 > 2\sigma(F^2)]$ = 0.023
$wR(F^2)$ = 0.048
S = 0.84
1495 reflections
99 parameters
0 restraints

Hydrogen site location: difference Fourier map
All H-atom parameters refined
$w = 1/[\sigma^2(F_o^2) + (0.0227P)^2]$
where $P = (F_o^2 + 2F_c^2)/3$
$(\Delta/\sigma)_{max} < 0.001$
$\Delta\rho_{max}$ = 0.32 e Å^{-3}
$\Delta\rho_{min}$ = −0.28 e Å^{-3}

Special details

Geometry. All esds (except the esd in the dihedral angle between two l.s. planes) are estimated using the full covariance matrix. The cell esds are taken into account individually in the estimation of esds in distances, angles and torsion angles; correlations between esds in cell parameters are only used when they are defined by crystal symmetry. An approximate (isotropic) treatment of cell esds is used for estimating esds involving l.s. planes.

Refinement. X-ray diffraction intensity data of 1</b->-5 were collected in the series of w-scans using Stoe IPDS2 image plate diffractometer operated with Mo Kα radiation at 150 (2) K. The multi-scan absorption corrections were applied for every collected data set (Blessing, 1987; Blessing, 1989). The structures were solved using dual-space methods within SHELXT and full-matrix least squares refinements were carried out within SHELXL-2018/3 via the WinGX program interface (Sheldrick, 2015). All non-hydrogen positions were located in the direct and the difference Fourier maps and refined using anisotropic displacement parameters.

Fractional atomic coordinates and isotropic or equivalent isotropic displacement parameters (Å^2)

	x	y	z	U_{iso}*/U_{eq}
Co1	0.500000	0.500000	0.500000	0.01256 (8)
C2	0.2691 (3)	0.89171 (17)	0.42726 (16)	0.0202 (4)
H2	0.1925 (19)	0.9647 (17)	0.43085 (18)	0.024*
O1	0.7373 (2)	0.54766 (10)	0.35744 (11)	0.0154 (2)
O3	0.2152 (2)	0.44396 (13)	0.34702 (12)	0.0171 (2)
O2	0.8152 (2)	0.70089 (11)	0.22067 (12)	0.0210 (3)
N1	0.3895 (3)	0.69131 (12)	0.46601 (13)	0.0149 (3)
C3	0.5145 (3)	0.73694 (15)	0.37229 (15)	0.0152 (3)
C4	0.7044 (3)	0.65913 (15)	0.31028 (15)	0.0143 (3)
C1	0.2359 (3)	0.78838 (15)	0.50138 (17)	0.0181 (3)
H1	0.129 (2)	0.78431 (18)	0.5645 (14)	0.022*
N2	0.4455 (3)	0.85818 (13)	0.34665 (14)	0.0198 (3)
H2A	0.5026 (15)	0.9055 (12)	0.2898 (14)	0.024*
H3A	0.198 (4)	0.368 (2)	0.337 (2)	0.031 (6)*
H3B	0.076 (5)	0.474 (2)	0.343 (2)	0.044 (7)*

Atomic displacement parameters (Å²)

	U^{11}	U^{22}	U^{33}	U^{12}	U^{13}	U^{23}
Co1	0.01397 (13)	0.01072 (13)	0.01381 (14)	0.00019 (14)	0.00483 (9)	0.00071 (15)
C2	0.0227 (8)	0.0161 (8)	0.0230 (9)	0.0064 (6)	0.0079 (7)	−0.0020 (7)
O1	0.0163 (5)	0.0121 (5)	0.0191 (6)	0.0018 (4)	0.0071 (4)	0.0022 (4)
O3	0.0152 (6)	0.0142 (6)	0.0221 (6)	0.0018 (5)	0.0032 (4)	−0.0036 (5)
O2	0.0254 (6)	0.0180 (6)	0.0224 (6)	0.0018 (5)	0.0129 (5)	0.0035 (5)
N1	0.0157 (6)	0.0134 (7)	0.0160 (6)	0.0007 (5)	0.0040 (5)	0.0004 (5)
C3	0.0158 (7)	0.0140 (8)	0.0161 (8)	0.0001 (6)	0.0033 (6)	0.0004 (6)
C4	0.0136 (7)	0.0146 (8)	0.0149 (8)	−0.0017 (6)	0.0025 (6)	−0.0011 (6)
C1	0.0170 (7)	0.0186 (8)	0.0203 (8)	0.0036 (6)	0.0084 (6)	−0.0017 (7)
N2	0.0264 (7)	0.0136 (7)	0.0210 (7)	0.0026 (5)	0.0088 (6)	0.0041 (6)

Geometric parameters (Å, º)

Co1—O3	2.0931 (11)	O3—H3A	0.81 (2)
Co1—O3^{i}	2.0931 (11)	O3—H3B	0.78 (2)
Co1—O1^{i}	2.1041 (12)	O2—C4	1.239 (2)
Co1—O1	2.1041 (12)	N1—C3	1.329 (2)
Co1—N1^{i}	2.1241 (13)	N1—C1	1.376 (2)
Co1—N1	2.1242 (13)	C3—N2	1.351 (2)
C2—N2	1.361 (2)	C3—C4	1.488 (2)
C2—C1	1.365 (2)	C1—H1	0.91 (2)
C2—H2	0.87 (2)	N2—H2A	0.86 (2)
O1—C4	1.2831 (19)		
O3—Co1—O3^{i}	180.0	Co1—O3—H3A	115.5 (14)
O3—Co1—O1^{i}	93.48 (5)	Co1—O3—H3B	117.2 (18)
O3^{i}—Co1—O1^{i}	86.52 (5)	H3A—O3—H3B	109 (2)
O3—Co1—O1	86.52 (5)	C3—N1—C1	105.88 (13)
O3^{i}—Co1—O1	93.48 (5)	C3—N1—Co1	109.07 (10)
O1^{i}—Co1—O1	180.0	C1—N1—Co1	145.04 (12)
O3—Co1—N1^{i}	89.83 (5)	N1—C3—N2	110.67 (14)
O3^{i}—Co1—N1^{i}	90.17 (5)	N1—C3—C4	121.65 (14)
O1^{i}—Co1—N1^{i}	79.55 (5)	N2—C3—C4	127.67 (15)
O1—Co1—N1^{i}	100.45 (5)	O2—C4—O1	124.67 (15)
O3—Co1—N1	90.17 (5)	O2—C4—C3	121.46 (15)
O3^{i}—Co1—N1	89.83 (5)	O1—C4—C3	113.87 (14)
O1^{i}—Co1—N1	100.45 (5)	C2—C1—N1	109.28 (15)
O1—Co1—N1	79.55 (5)	C2—C1—H1	125.4
N1^{i}—Co1—N1	180.0	N1—C1—H1	125.4
N2—C2—C1	106.45 (15)	C3—N2—C2	107.71 (15)
N2—C2—H2	126.8	C3—N2—H2A	126.1
C1—C2—H2	126.8	C2—N2—H2A	126.1
C4—O1—Co1	115.71 (10)		
C1—N1—C3—N2	−0.31 (16)	N1—C3—C4—O1	−1.3 (2)

Co1—N1—C3—N2	179.03 (10)	N2—C3—C4—O1	177.84 (14)
C1—N1—C3—C4	178.99 (14)	N2—C2—C1—N1	−0.45 (18)
Co1—N1—C3—C4	−1.67 (16)	C3—N1—C1—C2	0.47 (17)
Co1—O1—C4—O2	−175.67 (11)	Co1—N1—C1—C2	−178.44 (14)
Co1—O1—C4—C3	3.72 (15)	N1—C3—N2—C2	0.04 (17)
N1—C3—C4—O2	178.08 (14)	C4—C3—N2—C2	−179.21 (14)
N2—C3—C4—O2	−2.8 (2)	C1—C2—N2—C3	0.25 (18)

Symmetry code: (i) −*x*+1, −*y*+1, −*z*+1.

Hydrogen-bond geometry (Å, º)

D—H···*A*	*D*—H	H···*A*	*D*···*A*	*D*—H···*A*
C1—H1···O2^{ii}	0.91	2.44	3.347 (2)	172
N2—H2*A*···O1^{iii}	0.86	2.37	2.9824 (18)	129
N2—H2*A*···O3^{iii}	0.86	2.20	2.978 (2)	151
O3—H3*A*···O2^{iv}	0.81 (2)	1.87 (2)	2.6731 (18)	168 (2)
O3—H3*B*···O1^{v}	0.78 (2)	1.92 (3)	2.6963 (17)	173 (2)

Symmetry codes: (ii) *x*−1, −*y*+3/2, *z*+1/2; (iii) −*x*+1, *y*+1/2, −*z*+1/2; (iv) −*x*+1, *y*−1/2, −*z*+1/2; (v) *x*−1, *y*, *z*.

Diaquabis(1,3-oxazole-4-carboxylato-κ^2N,O^4)cobalt(II) (Co-4oxa)

Crystal data

$[Co(C_4H_2NO_3)_2(H_2O)_2]$
M_r = 319.09
Monoclinic, $P2_1/c$
a = 5.1664 (7) Å
b = 10.9879 (15) Å
c = 9.7550 (11) Å
β = 99.378 (10)°
V = 546.37 (12) Å^3
Z = 2
$F(000)$ = 322
D_x = 1.940 Mg m^{-3}
Mo $K\alpha$ radiation, λ = 0.71073 Å
Cell parameters from 2467 reflections
θ = 2.8–29.4°
μ = 1.61 mm^{-1}
T = 150 K
Rod, pink
0.20 × 0.11 × 0.11 mm

Data collection

Stoe IPDS2 diffractometer
Radiation source: fine-focus sealed tube
Detector resolution: 6.67 pixels mm^{-1}
ω–scans
Absorption correction: multi-scan (SORTAV; Blessing, 1995)
T_{min} = 0.942, T_{max} = 0.948
2995 measured reflections
1458 independent reflections
1104 reflections with $I > 2\sigma(I)$
R_{int} = 0.024
θ_{max} = 29.2°, θ_{min} = 2.8°
h = −7→6
k = −13→15
l = −13→12

Refinement

Refinement on F^2
Least-squares matrix: full
$R[F^2 > 2\sigma(F^2)]$ = 0.025
$wR(F^2)$ = 0.052
S = 0.91
1458 reflections
98 parameters
0 restraints
Hydrogen site location: difference Fourier map
All H-atom parameters refined
$w = 1/[\sigma^2(F_o^2) + (0.0281P)^2]$ where $P = (F_o^2 + 2F_c^2)/3$
$(\Delta/\sigma)_{max} < 0.001$
$\Delta\rho_{max}$ = 0.37 e Å^{-3}
$\Delta\rho_{min}$ = −0.28 e Å^{-3}

Special details

Geometry. All esds (except the esd in the dihedral angle between two l.s. planes) are estimated using the full covariance matrix. The cell esds are taken into account individually in the estimation of esds in distances, angles and torsion angles; correlations between esds in cell parameters are only used when they are defined by crystal symmetry. An approximate (isotropic) treatment of cell esds is used for estimating esds involving l.s. planes.

Refinement. X-ray diffraction intensity data of 1</b->-5 were collected in the series of w-scans using Stoe IPDS2 image plate diffractometer operated with Mo Kα radiation at 150 (2) K. The multi-scan absorption corrections were applied for every collected data set (Blessing, 1987; Blessing, 1989). The structures were solved using dual-space methods within SHELXT and full-matrix least squares refinements were carried out within SHELXL-2018/3 via the WinGX program interface (Sheldrick, 2015). All non-hydrogen positions were located in the direct and the difference Fourier maps and refined using anisotropic displacement parameters.

Fractional atomic coordinates and isotropic or equivalent isotropic displacement parameters (Å²)

	x	*y*	*z*	U_{iso}*/U_{eq}
Co1	0.500000	0.500000	0.500000	0.01187 (9)
O4	0.2663 (2)	0.88157 (11)	0.48213 (14)	0.0213 (3)
O1	0.7373 (2)	0.56802 (10)	0.36309 (13)	0.0152 (2)
O3	0.2083 (2)	0.46901 (12)	0.32952 (14)	0.0172 (3)
O2	0.8395 (2)	0.73459 (11)	0.25189 (14)	0.0186 (3)
N1	0.3868 (3)	0.68823 (13)	0.49404 (15)	0.0135 (3)
C3	0.5207 (3)	0.74931 (15)	0.40020 (18)	0.0141 (3)
C4	0.7136 (3)	0.68066 (14)	0.33175 (17)	0.0134 (3)
C1	0.2420 (3)	0.77044 (15)	0.53788 (19)	0.0168 (3)
H1	0.132 (2)	0.7548 (4)	0.6016 (14)	0.020*
C2	0.4451 (3)	0.86603 (16)	0.3935 (2)	0.0195 (4)
H2	0.4986 (14)	0.9211 (15)	0.3430 (13)	0.023*
H3A	0.194 (4)	0.398 (3)	0.303 (3)	0.031 (6)*
H3B	0.076 (5)	0.497 (3)	0.334 (3)	0.045 (7)*

Atomic displacement parameters (Å²)

	U^{11}	U^{22}	U^{33}	U^{12}	U^{13}	U^{23}
Co1	0.01175 (13)	0.01075 (13)	0.01405 (16)	−0.00006 (13)	0.00491 (10)	0.00083 (16)
O4	0.0268 (6)	0.0159 (6)	0.0239 (8)	0.0042 (5)	0.0124 (5)	0.0000 (5)
O1	0.0144 (5)	0.0127 (5)	0.0199 (7)	0.0010 (4)	0.0070 (5)	0.0009 (5)
O3	0.0139 (5)	0.0164 (7)	0.0213 (7)	0.0019 (4)	0.0028 (5)	−0.0044 (5)
O2	0.0201 (5)	0.0178 (6)	0.0207 (7)	0.0011 (4)	0.0111 (5)	0.0051 (5)
N1	0.0138 (6)	0.0146 (7)	0.0129 (8)	−0.0009 (5)	0.0043 (5)	0.0002 (5)
C3	0.0147 (7)	0.0152 (7)	0.0131 (9)	−0.0011 (5)	0.0044 (6)	0.0008 (6)
C4	0.0115 (7)	0.0154 (7)	0.0133 (9)	0.0001 (5)	0.0019 (6)	−0.0009 (6)
C1	0.0174 (7)	0.0170 (8)	0.0166 (9)	0.0001 (6)	0.0046 (7)	−0.0004 (7)
C2	0.0241 (8)	0.0162 (8)	0.0209 (10)	0.0005 (6)	0.0113 (7)	0.0021 (7)

Geometric parameters (Å, º)

Co1—O3^{i}	2.0823 (14)	O3—H3A	0.82 (3)
Co1—O3	2.0823 (14)	O3—H3B	0.76 (3)
Co1—O1^{i}	2.0928 (11)	O2—C4	1.2434 (19)

Co1—O1	2.0928 (11)	N1—C1	1.289 (2)
Co1—N1	2.1476 (14)	N1—C3	1.405 (2)
Co1—N1^{i}	2.1476 (14)	C3—C2	1.339 (2)
O4—C1	1.351 (2)	C3—C4	1.492 (2)
O4—C2	1.3753 (19)	C1—H1	0.93 (2)
O1—C4	1.2760 (19)	C2—H2	0.85 (2)
O3^{i}—Co1—O3	180.0	Co1—O3—H3B	115 (2)
O3^{i}—Co1—O1^{i}	88.38 (5)	H3A—O3—H3B	112 (3)
O3—Co1—O1^{i}	91.62 (5)	C1—N1—C3	104.80 (14)
O3^{i}—Co1—O1	91.62 (5)	C1—N1—Co1	146.70 (11)
O3—Co1—O1	88.38 (5)	C3—N1—Co1	108.47 (10)
O1^{i}—Co1—O1	180.00 (4)	C2—C3—N1	108.59 (14)
O3^{i}—Co1—N1	91.30 (5)	C2—C3—C4	132.31 (15)
O3—Co1—N1	88.71 (5)	N1—C3—C4	119.08 (14)
O1^{i}—Co1—N1	100.13 (4)	O2—C4—O1	124.94 (13)
O1—Co1—N1	79.87 (4)	O2—C4—C3	119.69 (14)
O3^{i}—Co1—N1^{i}	88.70 (5)	O1—C4—C3	115.36 (13)
O3—Co1—N1^{i}	91.29 (5)	N1—C1—O4	113.76 (14)
O1^{i}—Co1—N1^{i}	79.87 (5)	N1—C1—H1	123.1
O1—Co1—N1^{i}	100.13 (4)	O4—C1—H1	123.1
N1—Co1—N1^{i}	180.0	C3—C2—O4	107.97 (15)
C1—O4—C2	104.88 (13)	C3—C2—H2	126.0
C4—O1—Co1	117.13 (9)	O4—C2—H2	126.0
Co1—O3—H3A	115.2 (18)		
C1—N1—C3—C2	−0.3 (2)	C2—C3—C4—O1	179.7 (2)
Co1—N1—C3—C2	178.36 (13)	N1—C3—C4—O1	1.4 (2)
C1—N1—C3—C4	178.41 (16)	C3—N1—C1—O4	0.0 (2)
Co1—N1—C3—C4	−2.98 (17)	Co1—N1—C1—O4	−177.65 (16)
Co1—O1—C4—O2	−179.81 (13)	C2—O4—C1—N1	0.3 (2)
Co1—O1—C4—C3	1.07 (18)	N1—C3—C2—O4	0.4 (2)
C2—C3—C4—O2	0.6 (3)	C4—C3—C2—O4	−177.97 (17)
N1—C3—C4—O2	−177.72 (16)	C1—O4—C2—C3	−0.5 (2)

Symmetry code: (i) −*x*+1, −*y*+1, −*z*+1.

Hydrogen-bond geometry (Å, º)

D—H···*A*	*D*—H	H···*A*	*D*···*A*	*D*—H···*A*
C1—H1···O2^{ii}	0.93	2.27	3.1781 (19)	166
C2—H2···O3^{iii}	0.85	2.50	3.238 (2)	146
O3—H3*A*···O2^{iv}	0.82 (3)	1.88 (3)	2.6949 (18)	178 (2)
O3—H3*B*···O1^{v}	0.76 (3)	1.98 (3)	2.7333 (16)	175 (3)

Symmetry codes: (ii) *x*−1, −*y*+3/2, *z*+1/2; (iii) −*x*+1, *y*+1/2, −*z*+1/2; (iv) −*x*+1, *y*−1/2, −*z*+1/2; (v) *x*−1, *y*, *z*.